Substrate-Induced Conformational Changes of Melibiose Permease from Escherichia coli Studied by Infrared Difference Spectroscopy †

ARTICLE *in* BIOCHEMISTRY · APRIL 2005

Impact Factor: 3.02 · DOI: 10.1021/bi048301z · Source: PubMed

5 AUTHORS, INCLUDING:

Víctor A Lórenz-Fonfría
University of Valencia
64 PUBLICATIONS **525** CITATIONS
SEE PROFILE

Gérard Leblanc
Atomic Energy and Alternative Energies Com…
85 PUBLICATIONS **2,237** CITATIONS
SEE PROFILE

Esteve Padrós
Autonomous University of Barcelona
102 PUBLICATIONS **1,341** CITATIONS
SEE PROFILE

Substrate-Induced Conformational Changes of Melibiose Permease from *Escherichia coli* Studied by Infrared Difference Spectroscopy†

Xavier León,‡ Víctor A. Lórenz-Fonfría,‡ Raymonde Lemonnier,§ Gérard Leblanc,§ and Esteve Padrós*,‡

Unitat de Biofisica, Departament de Bioquímica i de Biologia Molecular, Facultat de Medicina, Universitat Autònoma de Barcelona, 08193 Bellaterra, Barcelona, Spain, and Laboratoire de Physiologie des Membranes Cellulaires−LRC-CEA 16V, Université de Nice Sophia-Antipolis and CNRS (UMR 6078), 06238, Villefranche sur Mer Cedex, France

Received August 7, 2004; Revised Manuscript Received December 24, 2004

ABSTRACT: Fourier transform infrared difference spectroscopy has been used to obtain information about substrate-induced structural changes of the melibiose permease (MelB) from *Escherichia coli* reconstituted into liposomes. Binding of the cosubstrate Na^+ gives rise to several peaks in the amide I and II regions of the difference spectrum Na^+·MelB minus H^+·MelB, that denote the presence of conformational changes in all types of secondary structures (α-helices, *β*-sheets, loops). In addition, peaks around 1400 and at 1740−1720 cm^{-1} are indicative of changes in protonation/deprotonation or in environment of carboxylic groups. Binding of the cosubstrate Li^+ produces a difference spectrum that is also indicative of conformational changes, but that is at variance as compared to that induced by Na^+ binding. To analyze the following transport steps, the melibiose permease with either H^+, Na^+, or Li^+ bound was incubated with melibiose. The difference spectra obtained by subtracting the spectrum cation·MelB from the respective complex cation·melibiose·MelB were roughly similar among them, but different from those induced by cation binding, and more intense. Therefore, major conformational changes that are induced during melibiose binding/substrate translocation, like those denoted by intense peaks at 1668 and 1645 cm^{-1}, are similar for the three cotransporting cations. Changes in the protonation state and/or in the environment of given carboxylic residues were also induced by melibiose−MelB interaction in the presence of cations.

The melibiose permease (MelB)[1] from *Escherichia coli* transports the disaccharide melibiose into the cell by using the transmembrane electrochemical gradient of Na^+, Li^+, or H^+ (*1*). MelB is a member of the large family of Na^+-solute symporters that is predicted to consist of 12 transmembrane α-helices with the N and C termini located in the cytoplasm (*2*−*4*). More direct evidence for the 12 transmembrane motif has been recently obtained upon 2D crystallization of MelB (*5*). Several works have allowed the determination of two regions responsible for cation binding and sugar binding, respectively. The cationic binding site appears to be located in the NH_2-terminal domain of the permease (*6*−*8*), whereas the sugar-binding site seems to be lined by the C-terminal helices IX and X (*9*, *10*). Site-directed mutagenesis has also been used to identify other important residues for binding and transport (*7*, *11*−*16*). In this way, it has been hypothesized that at least two loops are involved in the cotransport mechanism. Gwizdek et al. (*4*) showed that loop 4−5 is near or is a part of the cation-binding site, and a role for helix IV in connecting cation- and sugar-binding sites has been hypothesized (*17*). The highly conserved loop 10−11 containing several Asp and Glu residues has been implicated in the sugar binding/translocation (*18*). Similarly, cysteine-scanning mutagenesis has given a rough picture about the relative positions of some helices (*19*, *20*).

In this work we further investigated conformational changes involved in substrate binding and translocation aiming at learning, among other aspects, how the cosubstrate binding increases the melibiose affinity and how both substrates are translocated and released. The first demonstration of substrate-induced changes of MelB conformation was obtained by monitoring the fluorescence of tryptophan residues (*9*, *21*). In those works, it was pointed out that the changes in permease fluorescence reflect conformational changes occurring upon the formation of ternary sugar/cation/permease complexes. Furthermore, the analysis of fluorescence resonance energy transfer allowed the characterization of cooperative changes of the structure of the sugar-binding site or of its immediate vicinity induced by ion binding (*10*, *22*).

Later on, analysis of MelB secondary structure by deconvoluted Fourier transform infrared (FTIR) spectra indicated the presence of conformational changes upon substrate binding (*23*). This was corroborated by substrate-induced

† This work was supported by Grants Bio4-CT97-2119 from the European Commission (to G.L. and E.P.), Picasso 98127 (to G.L.), BMC2003-04941 from the Dirección General de Investigación (MCYT) and 1999SGR-0102 from the Direcció General de Recerca, DURSI (to E.P.).

* Corresponding author. E-mail: esteve.padros@uab.es. Phone: 935811870. Fax: 935811907.

‡ Universitat Autònoma de Barcelona.

§ Université de Nice Sophia-Antipolis.

[1] Abbreviations: MelB, melibiose permease; mel, melibiose (6-*O*-α-galactopyranosyl-D-glucose); ATR, attenuated total reflection; FTIR, Fourier transform infrared; Na^+·MelB, the complex formed by the melibiose permease and bound Na^+; Li^+·MelB, the complex formed by the melibiose permease and bound Li^+; mel·Na^+·MelB, the complex formed by the melibiose permease and bound Na^+ and melibiose; mel·Li^+·MelB, the complex formed by the melibiose permease and bound Li^+ and melibiose.

10.1021/bi048301z CCC: $30.25
Published on Web 02/11/2005

variations in the amount and the rate of proton/deuterium exchange (*24*). We have now chosen FTIR difference spectroscopy as a powerful and sensitive method to detect not only subtle conformational changes in the protein induced by substrate binding and translocation but also changes in the protonation state of ionizable side chains (*25*, *26*).

MATERIALS AND METHODS

Sample Preparation and Data Acquisition. MelB production and purification and preparation of MelB proteoliposomes were carried out as described (*24*). A sample of 20 μL of a proteoliposome suspension (about 150 μg of protein) was spread homogeneously on a germanium ATR crystal (50 × 10 × 2 mm, Harrick, Ossining, NY, yielding 12 internal reflections at the sample side) and dried under a stream of nitrogen. The substrate-containing buffer and the reference buffer (containing or not MelB substrates) were alternatively perfused over the proteoliposome film at a rate of ≈1.5 mL/min. The film was exposed to the substrate-containing buffer for 4 min and washed with the reference buffer for 10 min (15 min when the substrate-containing buffer had 50 mM melibiose). The switch of buffers was carried out by a computer-controlled electro valve. For each cycle, 500 scans at a resolution of 4 cm^{-1} were recorded and a total of 50 spectra were taken and averaged in order to increase the signal-to-noise ratio, i.e., a total of 25000 scans for every difference spectrum. Each experiment took about 10 h to be completed, and a minimum of two separate experiments using newly prepared films were done for each condition. Spectra were recorded with a FTS6000 Bio-Rad spectrometer, equipped with a mercury−cadmium−telluride detector. Sample temperature was adjusted to 20 °C using a cover jack placed over the ATR crystal and connected to a circulating thermostatic bath. The cover jack temperature was controlled with a fitted external probe.

Data Corrections. The experimental difference spectrum contains four possible contributions: (i) sample (protein and lipid) difference spectrum induced by the substrate(s); (ii) water difference spectrum induced by the substrate(s) (*27*); (iii) absorbance of the substrate(s) (in our case melibiose or saccharose, since the cations do not absorb); (iv) change in the swelling of the film, with an apparent gain/loss of water with a concomitant apparent loss/gain of sample (protein and lipid). The latter contribution was corrected by subtracting, from the experimental difference spectrum, an absorption spectrum of MelB proteoliposomes in the substrate-containing buffer. The subtraction factor used was that able to remove the lipid CH_2 bands at 2920 and 2850 cm^{-1}. Contributions ii and iii were corrected subtracting from the experimental difference spectrum a difference between the substrate-containing buffer and the reference buffer. The subtraction factor was adjusted to flatten the water band between 3700 and 2800 cm^{-1} and to remove bands coming from the substrates (melibiose and saccharose give an intense band at 1080 cm^{-1}, whereas cations give no bands).

Controls. Sample losses, temperature changes, or spectrometer instabilities can generate by their own fictitious bands in difference spectra. To evaluate these possible problems, we obtained differences for MelB films using the same buffer in both containers. No signal was observed in the difference spectrum, demonstrating the reliability of the experimental setup. Another control was to check that *E. coli* lipids do not produce difference spectra upon cation and/or melibiose interaction by their own. To this end, a film of *E. coli* lipids was spread on the germanium crystal, dried, and perfused with the corresponding buffers. After corrections, no bands were observed in the difference spectrum. Finally, to ascertain if the time exposure of the proteoliposome film to the substrate-containing buffer and posterior washing with buffer alone was long enough, the film was exposed to the substrate-containing buffer for 3, 10, 20, or 30 min and cleaned for 30 min with the reference buffer. No changes were observed between these differences, except for small perturbations in the baseline at the amide II region for longer time exposures.

Spectra Deconvolution. Deconvolution by the maximum entropy method was applied to difference spectra to resolve overlapped bands. Deconvolution strongly enhances the noise in the data. Therefore, for being applicable to real data, deconvolution must operate with some noise suppression. The most habitually used deconvolution method is Fourier deconvolution (FD), which discriminates between signal (noiseless data) and noise only on the basis of their frequency. This approach has two important limitations: (i) a frequency cut-point should be selected, making the result rather arbitrary; (ii) for some frequencies, signal and noise contributions are both significant, so we either dismiss available true signal or include important noise in the deconvolution result. Therefore, in FD we are constrained to obtain less narrowing and more noise enhancement than it is possible. On the other hand, maximum entropy deconvolution (MaxEntD) follows another approach for the discrimination of noise and signal. Signal is discriminated from noise on the basis of its property for describing the data while keeping the deconvolution solution simple, whereas noise does not. Data description is measured by chi-square function, whereas solution simplicity is measured by some entropy expression. In this way, we obtain the simplest deconvolution solution that is consistent with the data. It has been shown that MaxEntD outperforms FD, especially at low signal-to-noise conditions. Recently, we have introduced a new entropy expression that is particularly suited for the deconvolution of difference spectra (*28*). Deconvolution was performed using a Lorentzian band of 7 cm^{-1} width. This value was determined from the spectra as described (*29*). For the maximum entropy deconvolution, the same regularization parameter was used for all spectra. Its value was derived in accordance with the spectral noise content (*28*).

RESULTS

Na^+ and Li^+ Binding. Transport of melibiose by MelB can be coupled to Na^+, Li^+, or H^+ cotransport (*11*). Therefore, we first examined the changes induced by binding of the coupling ions Na^+ or Li^+, with reference to MelB with H^+ bound. Figure 1A shows the absorbance spectra of a film of MelB reconstituted with *E. coli* lipids, recorded in the presence and absence of Na^+. At first sight, the spectra are indistinguishable. Hence the difference spectrum Na^+·MelB vs H^+·MelB was computed (Figure 1B). The difference spectrum was found to be specific for interaction of the cotransported ion with the transporter, as neither addition of Ca^{2+} to MelB proteoliposomes nor Na^+ interaction with

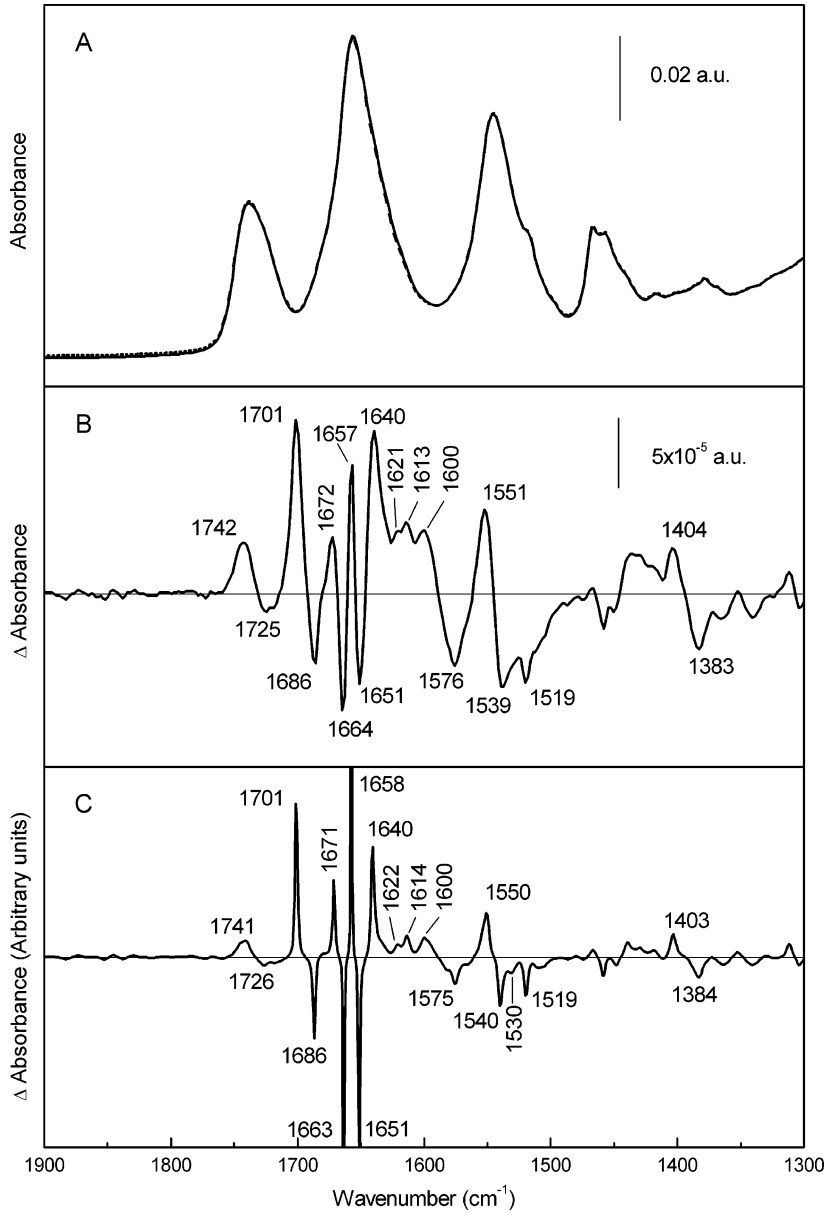

FIGURE 1: Absorption and difference spectra of Na^+·MelB and H^+·MelB. (A) ATR-FTIR absorption spectra of a rehydrated film of MelB in NaCl 10 mM, 20 mM MES, 100 mM KCl, pH 6.6 (Na^+·MelB, continuous black trace) or in 20 mM MES, 110 mM KCl, pH 6.6 (H^+·MelB, dashed gray trace), after buffer subtraction. A total of 25000 scans at a resolution of 4 cm^{-1} were averaged for each spectrum. (B) Difference between the spectra Na^+·MelB and H^+·MelB shown in panel A. (C) Deconvoluted spectrum of the difference shown in panel B.

a film of *E. coli* lipids alone produced significant spectral differences (data not shown). Although the majority of peaks in the difference spectrum of Figure 1B appear sufficiently narrow to presume that no overlapping between the peaks exists, the difference spectrum was deconvoluted to ensure that no band was overlooked, especially in the region 1640−1600 cm^{-1} (Figure 1C). The signal-to-noise ratio of the difference spectra is sufficiently high to admit deconvolution by the maximum entropy method (*28*), as evidenced by the low noise level above 1750 cm^{-1}. Fourier deconvolution gave similar spectra, albeit with higher noise (not shown). On the other hand, it should be noted that, since narrow bands are favored by deconvolution, broad bands are less prominent in the deconvoluted spectrum (e.g. the band at 1740 cm^{-1}). All deconvoluted difference spectra described in this work were highly reproducible.

Some peaks may reflect changes in the secondary structure whereas others may be due to changes in residue side chains. Additionally, there may be a likely lipid contribution to the spectral changes around 1740 cm^{-1} or below 1500 cm^{-1} that, for the sake of space, we will not consider. In the amide I region (1700−1610 cm^{-1}), large peaks are detected at 1658 and 1651 cm^{-1}, i.e. at the level of absorbance signals previously attributed to 2 distinct types of helical structures (type I and II, respectively (*23*)). It is striking that the two different helix signals vary in opposite directions (1658 (+); 1651 cm^{-1}(−)). The peak at 1640 cm^{-1} (+) may correspond to changes of β-sheet signal (*23*) whereas the intense peak at 1701 cm^{-1} (+) (*30*) and that at 1686 cm^{-1} (−) may reflect changes in the environment of reverse turns (*23*). Interpretation of the peak at 1663 cm^{-1} (−) is more difficult, as this position may correspond to signal variation arising either

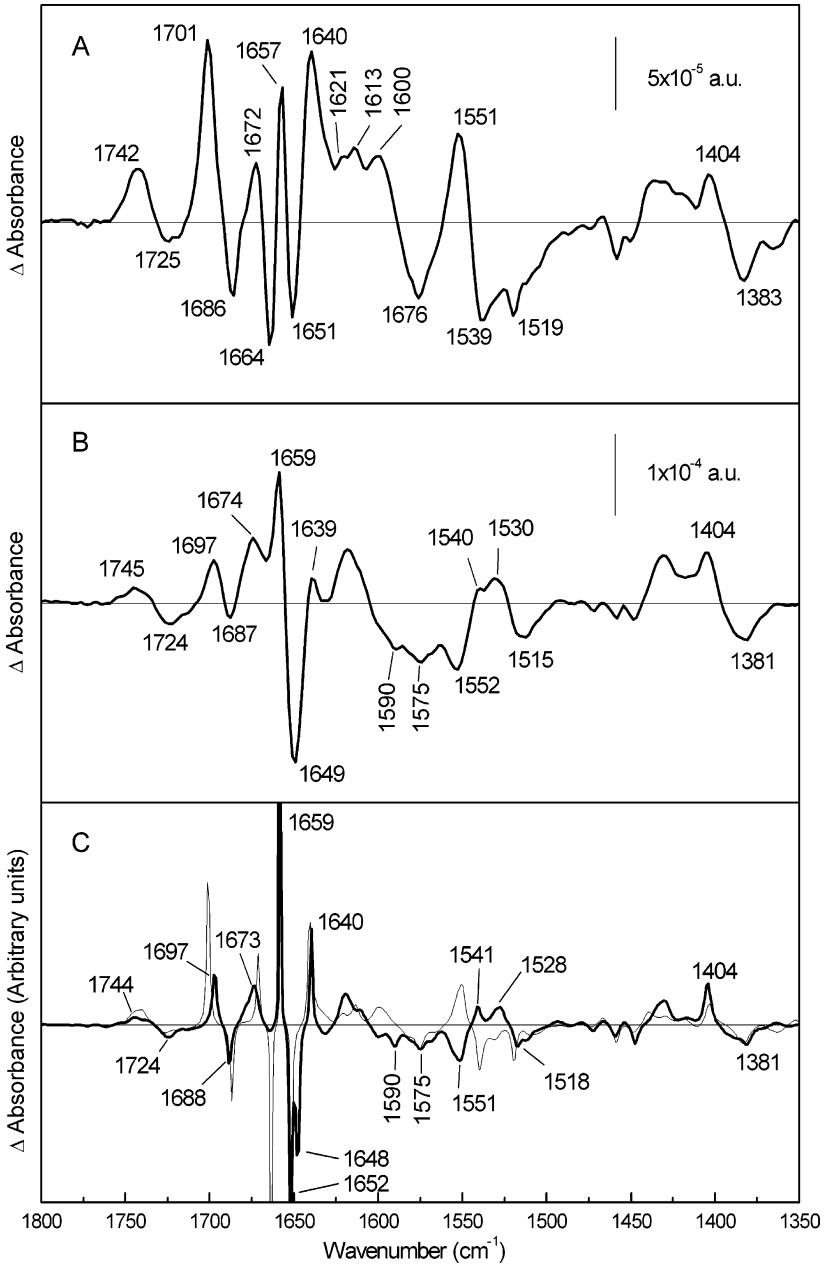

FIGURE 2: Difference spectra between cation·MelB and H^+·MelB. (A) Spectrum of the difference between Na^+·MelB and H^+·MelB shown in Figure 1B. (B) ATR-FTIR difference spectrum of a film of MelB in 10 mM LiCl, 20 mM MES, 100 mM KCl, pH 6.6, minus the film in 20 mM MES, 110 mM KCl, pH 6.6. A total of 25000 scans at a resolution of 4 cm^{-1} were averaged and subtracted. (C) Thick line: Deconvoluted spectrum of the difference between Li^+·MelB and H^+·MelB shown in panel B. Thin line: Deconvoluted spectrum of the difference between Na^+·MelB and H^+·MelB, shown in Figure 1C.

from α-helix or from loops (*31*). An additional indication of Na^+-induced change in MelB secondary structure is given by the appearance of the pair of peaks at 1550 (+) and 1540 cm^{-1} (−) in the amide II region (*26*). Of particular interest is to note that other spectral peaks suggest changes in the protonation state and/or environment of MelB acidic residues as well as change in the contribution of other side chain residues (*32*). Thus, the peaks at 1403 (+, COO^- symmetric vibrations) and 1726 cm^{-1} (−, COOH stretching) can be due to deprotonation of carboxylic acids, while that at 1701 cm^{-1} may also contain contribution from protonation of other carboxylic side chains (*33*). However, the two pair of peaks at 1403 (+)/1384 cm^{-1} (−) and at 1741(+)/1726 (−) cm^{-1} may indicate changes in the environment of deprotonated and protonated carboxylic acids, respectively (*32*). One may note that perturbations of lipid esters interacting with the protein may well contribute the peak at 1741 cm^{-1} (+) (*34*). In addition to these changes, the possibility that Na^+ binding induces changes in Tyr side chain signal is suggested by the negative peak at 1519 cm^{-1}, whereas changes in Arg side chain may give rise to the peak at 1671 cm^{-1} (*26*, *32*). More ambiguous are the small peaks at 1622 and 1614 cm^{-1} which might be a mixture of changes in the properties of Asn, Gln, Trp, or Tyr side chains (*32*) and of MelB β-sheet components.

Figure 2 shows the difference and the corresponding deconvoluted spectra induced by Li^+ binding, and their comparison to those induced by Na^+ binding. It is apparent that the changes produced by Li^+ binding partly differ from those of Na^+ binding. According to Figure 2C, some peaks have similar position and sign in both Na^+- and Li^+-difference spectra, namely those at 1688(−), 1673(+), 1659-

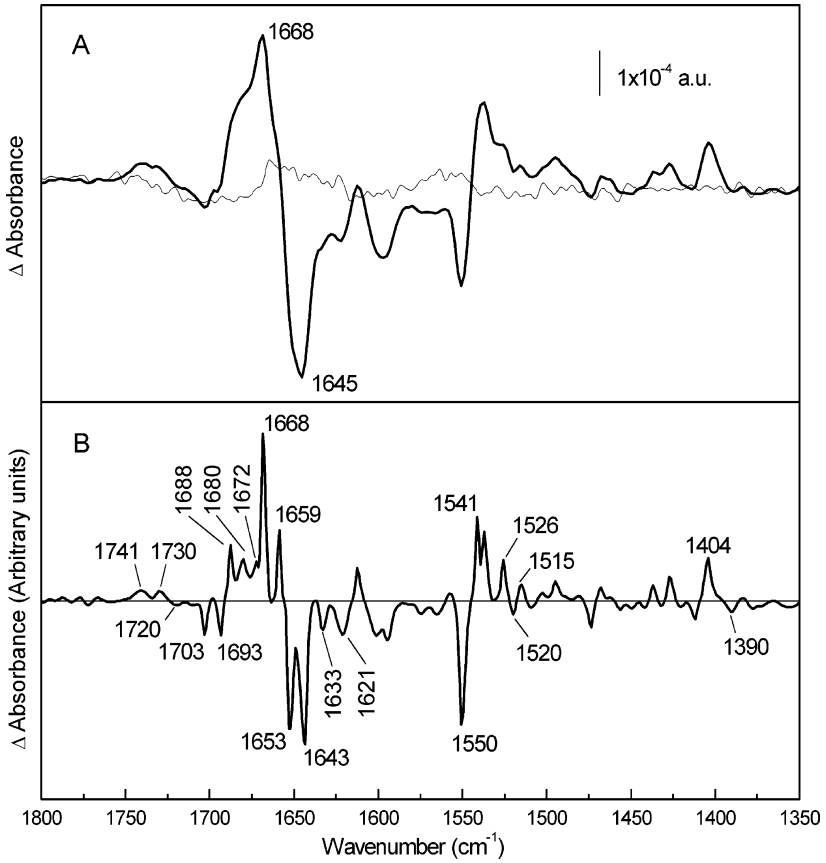

FIGURE 3: Difference spectrum between mel·Na^+·MelB and Na^+·MelB. (A) Thick line: ATR-FTIR difference spectrum of a film of MelB in 20 mM MES, 100 mM KCl, 10 mM NaCl, 10 mM melibiose, pH 6.6, minus the film in 20 mM MES, 100 mM KCl, 10 mM NaCl, pH 6.6. Thin line: ATR-FTIR difference spectrum of a film of MelB in 20 mM MES, 100 mM KCl, 10 mM NaCl, 10 mM saccharose, pH 6.6, minus the film in 20 mM MES, 100 mM KCl, 10 mM NaCl. This spectrum shows a decreased signal-to-noise ratio because only 12000 scans were accumulated. (B) Deconvoluted spectrum of the difference between mel·Na^+·MelB and Na^+·MelB shown in panel A.

(+), 1652(−), and 1640 (+) cm^{-1}. In contrast, the positive peak at 1701(+) cm^{-1} in the Na^+-induced spectrum is replaced by a peak at 1697 (+) cm^{-1} in the Li^+-induced spectrum. The negative peak at 1663 cm^{-1} of the Na^+ spectrum does not have a correspondence in the Li^+ spectrum, whereas the negative peak at 1648 cm^{-1} induced by Li^+ is not seen in the Na^+ spectrum. In the amide II region, the difference spectra are noticeably at variance. Na^+ or Li^+ binding induces similar peaks at 1575 (−) and 1518 cm^{-1} (−), but the rest of the peaks have no correspondence; moreover, most of them appear to be of opposite sign, as those at 1600 (+), 1550 (+), 1540 (−), and 1530 cm^{-1} (−) for Na^+; and 1590 (−), 1551 (−), 1541 (+), and 1528 cm^{-1} (+) for Li^+. These latter spectral variations illustrate that Na^+ and Li^+ binding may affect differently the structure of the transporter.

Melibiose Interaction in the Presence of Na^+. After cation binding, the next step in the MelB transport cycle is melibiose binding (*35*). However, as substrate translocation occurs when both cosubstrates are bound to melB, the difference spectrum mel·Na^+·MelB vs Na^+·MelB presented in Figure 3A (black trace) reflects not only events associated with sugar binding but also those linked to cosubstrate translocation. Possible unspecific contributions of sugar binding can be discarded as (i) saccharose, that is not a substrate of MelB, does not elicit the appearance of spectral peaks (Figure 3A, gray trace), and (ii) the difference spectrum obtained using the alternative substrate β-galactoside instead of melibiose was very similar to that of melibiose (data not shown).

Figure 3A (black trace) shows the melibiose-induced difference spectrum (mel·Na^+·MelB vs Na^+·MelB) together with its deconvolution (Figure 3B). The signal variations appear more intense than those elicited by Na^+ or Li^+ binding, suggesting that melibiose induces greater conformational changes than binding of cation alone. Several peaks are observed, again reflecting changes in both the secondary structure and amino acid side chains of the transporter. The peaks centered at 1659 (+) and 1653 cm^{-1} (−), as in the Na^+·MelB vs H^+·MelB spectrum, suggest changes in α-helix signals. Therefore, even if these structures already change upon Na^+ binding, melibiose binding/substrate translocation produces additional changes. The main peak at 1668 cm^{-1} (+), not seen in the difference spectrum due to Na^+ binding, is expected to reflect changes in turns or in open loop signals. The peak centered at 1643 cm^{-1} (−), resolved by deconvolution, is of difficult assessment (β-sheets, 3_{10} helices or open loops; see ref *23*). Bands appearing at 1680 (+) and 1672 (+) cm^{-1} may correspond to Gln, Asn, or Arg side chains (*31*, *32*, *36*). The other bands in the amide I region may correspond to changes in β-sheets or in side chains (1693 (−), 1633 (−), 1621 (−) cm^{-1}) (*32*, *37*) and turns (1688 (+), 1703(−) cm^{-1} (*30*)). In the amide II, the principal peaks are consistent with the assignment to helices and sheets (1550 and 1541 cm^{-1}, respectively) (*38*). Another band at 1526 cm^{-1} (+) could be assigned to perturbation of lysine side chains (*37*) whereas that at 1515 cm^{-1} may be due to Tyr residues. On comparing the difference spectrum induced by melibiose with that induced by Na^+, it is worth noting that

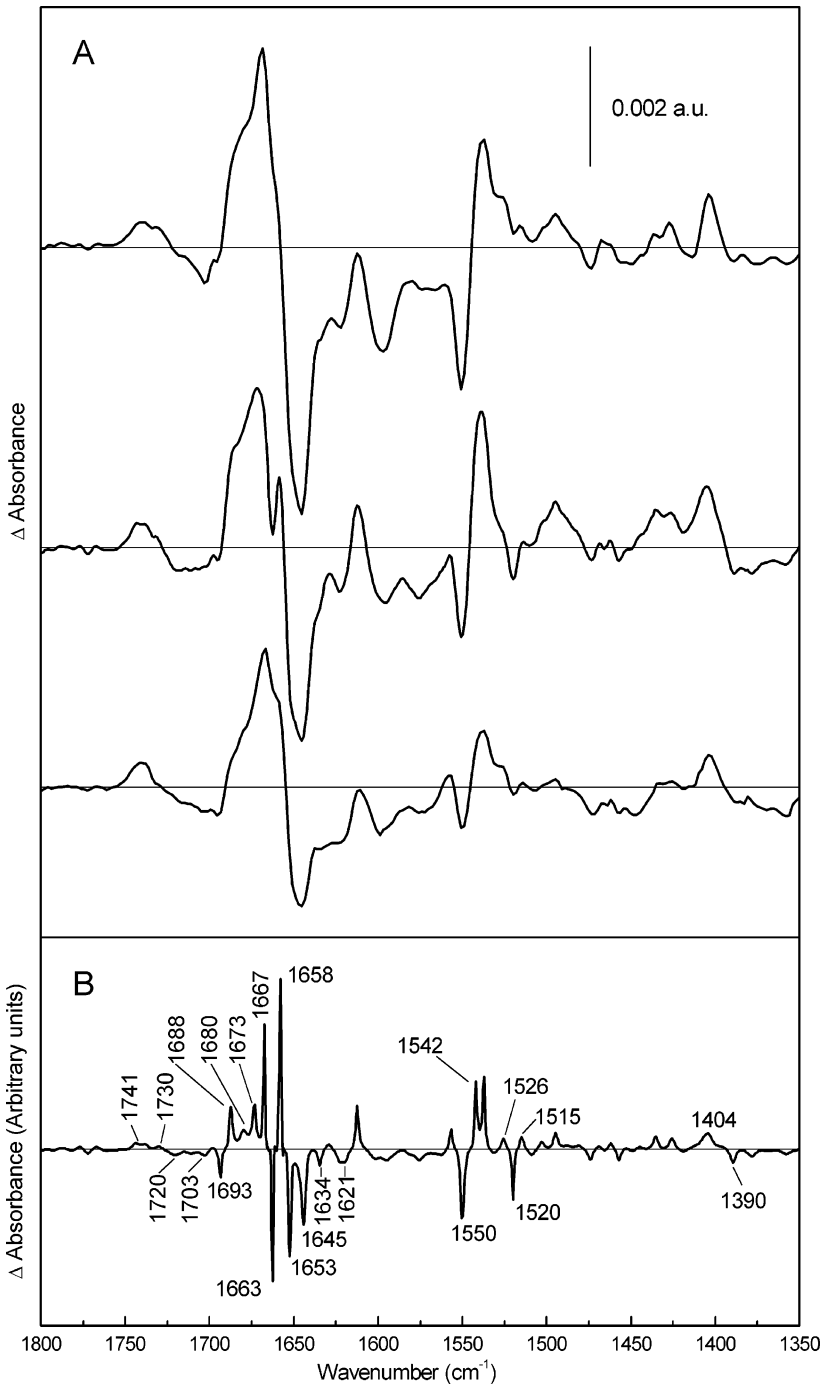

FIGURE 4: Difference spectra of melibiose binding in the presence of cations. (A) Top: Spectrum of the difference between mel·Na^+·MelB and Na^+·MelB shown in Figure 3A. Middle: ATR-FTIR difference spectrum of a film of MelB in 20 mM MES, 100 mM KCl, 10 mM LiCl, 10 mM melibiose, pH 6.6, minus the film in 20 mM MES, 100 mM KCl, 10 mM LiCl, pH 6.6. Bottom: ATR-FTIR difference spectrum of a film of MelB in 20 mM MES, 100 mM KCl, 50 mM melibiose, pH 6.6, minus the film in 20 mM MES, 100 mM KCl, pH 6.6. (B) Deconvoluted spectrum of the difference between mel·Li^+·MelB and Li^+·MelB shown in panel A, middle.

several bands in both amide I and II regions that are located at similar wavenumbers have opposite signs (peaks at 1703, 1688, 1550, and 1541 cm^{-1} of the Na^+·melibiose difference spectrum). This suggests that the changes of these structures produced by Na^+ binding are reversed by melibiose binding/substrate translocation.

As in the spectrum of Na^+ binding, a positive peak at 1404 cm^{-1} is observed, which can be due to deprotonation of carboxylic acids. This peak, or at least part of it, taken together with the negative peak at 1390 cm^{-1}, may indicate a change in the environment of a deprotonated carboxylic acid (*32*). Above 1700 cm^{-1}, there are two positive peaks well above the noise at 1741 and 1730 cm^{-1}. As in the case of Na^+-induced spectrum, it seems plausible that these peaks correspond to protonation of Asp or Glu side chains.

Melibiose Interaction in the Presence of Li^+ or H^+. Figure 4A shows the difference spectra induced by melibiose interaction in the presence of either Na^+, Li^+, or H^+. The 3 spectra reveal a rough similarity, indicating that the conformational changes induced by melibiose binding/substrates translocation are comparable, irrespective of the bound cation. However, specific variations are worth noting. Figure 4A (middle trace) shows the difference spectrum mel·Li^+·MelB vs Li^+·MelB. In the corresponding deconvoluted

difference spectrum (Figure 4B), a negative band centered at 1663 cm^{-1} is clearly seen that does not appear in the difference spectrum caused by melibiose in the presence of either H^+ or Na^+, nor in the difference spectrum due to Li^+ binding. This peak is an indication of distinct conformational changes triggered by melibiose interaction in the presence of Li^+, as compared to melibiose interaction in the presence of Na^+. Other differences are the peak at 1703 cm^{-1}, that has lower intensity in the mel·Li^+·MelB vs Li^+·MelB, and the peak at 1520 cm^{-1} in the amide II, that is less intense in the mel·Na^+·MelB vs Na^+·MelB spectrum.

DISCUSSION

In agreement with our preliminary FTIR spectroscopy observation suggesting substrate-induced change in the absorbance of MelB (*23*), the infrared difference spectral analysis carried out in this work shows multiple and discrete absorbance changes (in the range 1740−1400 cm^{-1}) of the MelB transporter associated with binding of the cosubstrates and/or with their transport. Taking data from the literature (*38*) and from previous FTIR studies on MelB (*23*), some of the sharp peaks observed at specific wavenumbers were assigned to conformational changes occurring at the level of the major structural components of MelB (α-helices, *β*-sheets, turns). The data also reveal substrate-induced changes in side chain properties of some acidic and tyrosyl residues, in particular.

To better appreciate the importance of these discrete absorbance changes, it is useful to relate them to the different kinetic intermediates included in the 6-state model which satisfactorily describe the major kinetic properties of MelB and which rely on the postulate of an alternating access to the substrate binding sites (*11*, *35*). Briefly summarized, upon addition of Na^+ (or Li^+) at saturating concentration, cation binding gives rise to cation-MelB species at the expense of preexisting H^+·MelB ones (*35*). As MelB does not transport the coupling ion in the absence of sugar, the cation-MelB species should predominate and be mostly outwardly oriented. In the presence of melibiose and either H^+ or Na^+ or Li^+, MelB cycles through six conformational intermediates assumed in its transport (*35*), partly outwardly or inwardly oriented. As the concentration of each cosubstrate is saturating, most of the transporters have both substrates bound (mel·cation·MelB species) and in the two orientations. Therefore, the melibiose-induced difference spectrum most likely monitors the conformational changes resulting from sugar binding (in the presence of bound cation) merged with a certain percentage of translocation of the ternary complex.

Changes Induced by Na^+ or Li^+ Binding. Binding of Na^+ to MelB produces a set of positive and negative peaks in the amide I and II regions, that are due to changes in secondary and tertiary structures, as well as to changes in the environment or in the protonation state of some side chains. Most of the peaks can be assigned to changes of several kinds of secondary structures that produce shifts in the corresponding absorption bands, giving rise to pairs of contiguous positive/negative peaks in the difference spectrum. For this reason, significant conversion of a type of secondary structure to a different type does not seem to exist.

Changes in α-helices are indicated by the peaks at 1658 (+) and 1651 cm^{-1} (−). This is in keeping with the previous description of two types of α-helices absorbing at 1660 and 1653 cm^{-1} (*23*). It was already noted that incubation of MelB with the substrate Na^+ induced small changes in the deconvoluted bands corresponding to these helices (*23*). Because the two peaks of the difference spectrum have different sign, a possibility exists that there is an interconversion between the helices absorbing at 1651 and at 1658 cm^{-1}. A second possibility is that these peaks are due to opposite changes in helix orientation. As the proteoliposomes have a net orientation in the film, change of helical orientation will change the intensity of the helical band (*39*).

Of interest is the positive peak at 1403 cm^{-1}, that can be due to the COO^- group of Glu or Asp side chains, i.e., to a deprotonation of these group(s). Because it is accompanied by a contiguous negative peak at 1384 cm^{-1}, it can instead correspond to a change in the environment of an already deprotonated group. Deprotonation of a carboxylate group is also suggested by the appearance of a small negative peak at 1726 cm^{-1}. In this region, the peak at 1741 cm^{-1} may correspond to lipid ester carbonyl groups, but a carboxyl protonation can also contribute in this wavenumber. It is even possible that both contribute, the resulting peak being a mixture of both (see Figure 1B as an example). If this is the case, then the peak at 1741 cm^{-1} or part of it (meaning appearance of a protonated carboxyl group) could have its counterpart in the negative peak at 1384 cm^{-1} (meaning disappearance of a deprotonated group). In any case, the peaks corresponding to carboxylic groups are of great interest because it has been previously shown that several Asp and Glu side chains are required for Na^+ binding and melibiose transport (*7*, *18*, *40*). Furthermore, bands near 1671 cm^{-1} may be assigned to Arg side chain. This would agree with the proposed existence of salt bridges near the ion binding site, such as the ones between Arg52 and Asp19 or Asp55 or Lys 377 and Asp 59 (*41*). Future work with MelB mutants will be necessary in order to identify the individual amino acid(s) causing these peaks.

As described in the Results, Li^+ binding also induces a typical difference spectrum that partly differs from that induced by Na^+ binding. From studies on the kinetics of substrate translocation (*11*), it was suggested that the complexes involving melibiose and Li^+ are more stable than those involving melibiose and Na^+. The variations in the respective difference spectra induced by the binding of each of these two cations may reflect this fact.

Changes Induced by Melibiose Interaction. The difference spectra induced by melibiose incubation in the presence of Na^+, Li^+, or H^+ are comparable (see Figure 4), indicating that the protein changes induced by melibiose binding/substrates translocation are roughly similar in the three conditions. However, some dissimilarities do exist that should reflect the different kinetic properties of melibiose binding/transport under a Na^+, Li^+, or H^+ gradient (*42*). On the other hand, the sugar-induced difference spectra show an amplitude about three times larger than those observed upon binding of Na^+ or Li^+ alone, demonstrating that the changes induced by melibiose interaction are proportionally larger than the ion-induced ones. This conclusion is consistent with the previous observation of a greater protection against hydrogen/deuterium exchange by melibiose than by Na^+ ions (*24*). When relating these results to the six-state model for transport it seems logical in terms of the conformational changes

inherent to the transport process. In the first step, binding of the cation should give rise to (relatively small) conformational changes that will increase the affinity of the transporter for the sugar. In the second step, binding of the sugar will lead to bigger conformational changes, as the transporter should switch its aperture from the extracellular to the cytoplasmic space. This mechanism most probably includes a variety of conformational changes but also helical tilting. In fact, changes in the orientation of helices have been described or suggested during the switching mechanism of the bacterial oxalate transporter OxlT (*43*) and for the lactose permease (*44*). These changes in orientation may not necessarily encompass the full length of helices, but may be in some cases restricted to part of them (*43*). On the other hand, the switching mechanism for MelB may also involve the movement of one putative reentrant loop (loop 10−11 (*45*)) or one putative mobile loop (loop 4−5 (*16*)). This would produce peaks in the difference spectra due to changes in environment and/or protonation changes of carboxylic side chains present in these loops.

Among the peaks produced by melibiose, those at 1404/1390 cm^{-1} and 1741, 1729/1720 cm^{-1} may indicate protonation/deprotonation reactions and/or changes in the environment of carboxylic groups, as pointed out in Results. Therefore, while Na^+ or Li^+ binding already originates protonation/deprotonation and/or environmental changes of Asp or Glu side chains, melibiose binding/substrate translocation produces additional changes of the same or different carboxyl groups. Here, it can be recalled that cation binding is affected by acidic residues located on helices II−IV (*7*) whereas sugar binding/translocation depends on acidic residues on loops 4−5 and 10−11 (*45*, *46*). Therefore, one is tempted to relate the peaks in the cation-induced difference spectra to carboxylic side chains on helices II−IV and those due to sugar binding to acidic side chains located on the major loops 4−5 and 10−11. It could also happen that some acidic side chains perturbed by cation binding suffer additional changes induced by sugar binding/translocation. Moreover, as already pointed out above, peaks observed around 1672 cm^{-1} may be due to Arg side chains. The proposed salt bridges between Arg52 with Asp19 and Asp55 or Asp59 and Lys377 could break during the catalytic mechanism (*41*), thus giving rise to peaks in the difference spectrum. Arg141 is another side chain important for melibiose translocation (*16*) that may become altered and produce peaks.

A positive peak at 1515 cm^{-1}, that can be attributed to Tyr side chains, appears in all difference spectra induced by melibiose, whereas cation binding produces negative peaks at 1518−1519 cm^{-1} that could also be attributed to Tyr side chains. This is in keeping with site-directed mutagenesis studies showing alterations in substrate binding/transport on mutation of some Tyr side chains (*13*). As has been previously suggested, the putative cationic binding site contains several Tyr that may participate directly or indirectly in the binding of cations (*13*).

Despite the mentioned particularities, it is of interest to stress the close similarity of the difference spectra induced by melibiose incubation in the presence of either coupling ion. This indicates that the fundamental trends inherent to the mechanism of binding and cotransport of melibiose and any of the coupling ions remain very similar. Taken together, the data presented in this work provide evidence for conformational changes characteristic of some steps of the transport cycle of the MelB permease. These comprise cation binding and sugar binding/substrate translocation. On the basis of these results, future work aimed at the identification of the peaks in the difference spectra, using in particular MelB mutants and/or studies in D_2O, should provide clues about the molecular mechanism of ion-coupled sugar symport.

ACKNOWLEDGMENT

We thank Dr. Natàlia Dave for helpful discussions and suggestions.

REFERENCES

1. Cohn, D. E., and Kaback, H. R. (1980) Mechanism of the melibiose porter in membrane vesicles of *Escherichia coli*, *Biochemistry 19*, 4237−4243.
2. Botfield, M. C., and Wilson, T. H. (1989) Peptide-specific antibody for the melibiose carrier of *Escherichia coli* localizes the carboxyl terminus to the cytoplasmic face of the membrane, *J. Biol. Chem. 264*, 11649−11652.
3. Pourcher, T., Bibi, E., Kaback, H. R., and Leblanc, G. (1996) Membrane topology of the melibiose permease of *Escherichia coli* studied by melB-phoA fusion analysis, *Biochemistry 35*, 4161−4168.
4. Gwizdek, C., Leblanc, G., and Bassilana, M. (1997) Proteolytic mapping and substrate protection of the *Escherichia coli* melibiose permease, *Biochemistry 36*, 8522−8529.
5. Hacksell, I., Rigaud, J. L., Purhonen, P., Pourcher, T., Hebert, H., and Leblanc, G. (2002) Projection structure at 8 Å resolution of the melibiose permease, an Na-sugar co-transporter from *Escherichia coli*, *EMBO J. 21*, 3569−3574.
6. Hama, H., and Wilson, T. H. (1993) Cation-coupling in chimeric melibiose carriers derived from *Escherichia coli* and *Klebsiella pneumoniae*. The amino-terminal portion is crucial for Na^+ recognition in melibiose transport, *J. Biol. Chem. 268*, 10060−10065.
7. Pourcher, T., Zani, M. L., and Leblanc, G. (1993) Mutagenesis of acidic residues in putative membrane-spanning segments of the melibiose permease of *Escherichia coli*. I. Effect on Na(+)-dependent transport and binding properties, *J. Biol. Chem. 268*, 3209−3215.
8. Wilson, D. M., and Wilson, T. H. (1992) Asp-51 and Asp-120 are important for the transport function of the *Escherichia coli* melibiose carrier, *J. Bacteriol. 174*, 3083−3086.
9. Mus-Veteau, I., and Leblanc, G. (1996) Melibiose permease of *Escherichia coli*: structural organization of cosubstrate binding sites as deduced from tryptophan fluorescence analyses, *Biochemistry 35*, 12053−12060.
10. Cordat, E., Mus-Veteau, I., and Leblanc, G. (1998) Structural studies of the melibiose permease of *Escherichia coli* by fluorescence resonance energy transfer. II. Identification of the tryptophan residues acting as energy donors, *J. Biol. Chem. 273*, 33198−33202.
11. Pourcher, T., Bassilana, M., Sarkar, H. K., Kaback, H. R., and Leblanc, G. (1990) The melibiose/Na^+ symporter of *Escherichia coli*: kinetic and molecular properties, *Philos. Trans. R. Soc. London, Ser. B: Biol. Sci. 326*, 411−423.
12. Pourcher, T., Deckert, M., Bassilana, M., and Leblanc, G. (1991) Melibiose permease of *Escherichia coli*: mutation of aspartic acid 55 in putative helix II abolishes activation of sugar binding by Na^+ ions, *Biochem. Biophys. Res. Commun. 178*, 1176−1181.
13. Zani, M. L., Pourcher, T., and Leblanc, G. (1994) Mutation of polar and charged residues in the hydrophobic NH2-terminal domains of the melibiose permease of *Escherichia coli*, *J. Biol. Chem. 269*, 24883−24889.
14. Franco, P. J., and Wilson, T. H. (1996) Alteration of Na(+)-coupled transport in site-directed mutants of the melibiose carrier of *Escherichia coli*, *Biochim. Biophys. Acta 1282*, 240−248.
15. Hastings Wilson, T., and Wilson, D. M. (1998) Evidence for a close association between helix IV and helix XI in the melibiose carrier of *Escherichia coli*, *Biochim. Biophys. Acta 1374*, 77−82.

16. Abdel-Dayem, M., Basquin, C., Pourcher, T., Cordat, E., and Leblanc, G. (2003) Cytoplasmic loop connecting helices IV and V of the melibiose permease from *Escherichia coli* is involved in the process of Na^+-coupled sugar translocation, *J. Biol. Chem. 278*, 1518−1524.
17. Cordat, E., Leblanc, G., and Mus-Veteau, I. (2000) Evidence for a role of helix IV in connecting cation- and sugar-binding sites of *Escherichia coli* melibiose permease, *Biochemistry 39*, 4493−4499.
18. Ding, P. Z. (2003) An investigation of cysteine mutants on the cytoplasmic loop X/XI in the melibiose transporter of *Escherichia coli* by using thiol reagents: implication of structural conservation of charged residues, *Biochem. Biophys. Res. Commun. 307*, 864−869.
19. Ding, P. Z., and Wilson, T. H. (2000) The melibiose carrier of *Escherichia coli*: cysteine substitutions for individual residues in helix XI, *J. Membr. Biol. 174*, 135−140.
20. Ding, P. Z., Weissborn, A. C., and Wilson, T. H. (2001) Cysteine substitutions for individual residues in helix VI of the melibiose carrier of *Escherichia coli*, *J. Membr. Biol. 183*, 33−38.
21. Mus-Veteau, I., Pourcher, T., and Leblanc, G. (1995) Melibiose permease of *Escherichia coli*: substrate-induced conformational changes monitored by tryptophan fluorescence spectroscopy, *Biochemistry 34*, 6775−6783.
22. Maehrel, C., Cordat, E., Mus-Veteau, I., and Leblanc, G. (1998) Structural studies of the melibiose permease of *Escherichia coli* by fluorescence resonance energy transfer. I. Evidence for ion-induced conformational change, *J. Biol. Chem. 273*, 33192−33197.
23. Dave, N., Troullier, A., Mus-Veteau, I., Duñach, M., Leblanc, G., and Padrós, E. (2000) Secondary structure components and properties of the melibiose permease from *Escherichia coli*: a Fourier transform infrared spectroscopy analysis, *Biophys. J. 79*, 747−755.
24. Dave, N., Lórenz-Fonfría, V. A., Villaverde, J., Lemonnier, R., Leblanc, G., and Padrós, E. (2002) Study of amide-proton exchange of *Escherichia coli* melibiose permease by attenuated total reflection-Fourier transform infrared spectroscopy: evidence of structure modulation by substrate binding, *J. Biol. Chem. 277*, 3380−3387.
25. Zscherp, C., Schlesinger, R., Tittor, J., Oesterhelt, D., and Heberle, J. (1999) In situ determination of transient pKa changes of internal amino acids of bacteriorhodopsin by using time-resolved attenuated total reflection Fourier transform infrared spectroscopy, *Proc. Natl. Acad. Sci. U.S.A. 96*, 5498−5503.
26. Baenziger, J. E., Miller, K. W., and Rothschild, K. J. (1993) Fourier transform infrared difference spectroscopy of the nicotinic acetylcholine receptor: evidence for specific protein structural changes upon desensitization, *Biochemistry 32*, 5448−5454.
27. Venyaminov, S. Y., and Kalnin, N. N. (1990) Quantitative IR spectrophotometry of peptides compounds in water (H_2O) solutions. I. Spectral parametres of amino acid residue absorption band, *Biopolymers 30*, 1243−1257.
28. Lórenz-Fonfría, V. A., and Padrós, E. (2005) Maximum entropy deconvolution of infrared spectra: Use of a novel entropy expression without sign-restriction, *Appl. Spectrosc*., in press.
29. Saarinen, P. E., Kauppinen, J. K., and Partanen, J. O. (1995) New method for spectral line shape fitting and critique on the Voight line shape, *Appl. Spectrosc. 49*, 1438−1453.
30. Krimm, S., and Bandekar, J. (1986) Vibrational spectroscopy and conformation of peptides, polypeptides, and proteins, *Adv. Protein. Chem. 3*, 181−364.
31. Troullier, A., Gerwert, K., and Dupont, Y. (1996) A time-resolved Fourier transformed infrared difference spectroscopy study of the sarcoplasmic reticulum Ca(2+)-ATPase: kinetics of the high-affinity calcium binding at low temperature, *Biophys. J. 71*, 2970−2983.
32. Barth, A. (2000) The infrared absorption of amino acid side chains, *Prog. Biophys. Mol. Biol. 74*, 141−173.
33. Furutani, Y., Kandori, H., and Shichida, Y. (2003) Structural changes in lumirhodopsin and metarhodopsin I studied by their photoreactions at 77 K, *Biochemistry 42*, 8494−8500.
34. DeGrip, W. J., Gray, D., Gillespie, J., Bovee, P. H., Van den Berg, E. M., Lugtenburg, J., and Rothschild, K. J. (1988) Photoexcitation of rhodopsin: conformation changes in the chromophore, protein and associated lipids as determined by FTIR difference spectroscopy, *Photochem. Photobiol. 48*, 497−504.
35. Bassilana, M., Pourcher, T., and Leblanc, G. (1988) Melibiose permease of *Escherichia coli*. Characteristics of co-substrates release during facilitated diffusion reactions, *J. Biol. Chem. 263*, 9663−9667.
36. Baenziger, J. E., and Chew, J. P. (1997) Desensitization of the nicotinic acetylcholine receptor mainly involves a structural change in solvent-accessible regions of the polypeptide backbone, *Biochemistry 36*, 3617−3624.
37. von Germar, F., Barth, A., and Mäntele, W. (2000) Structural changes of the sarcoplasmic reticulum Ca(2+)-ATPase upon nucleotide binding studied by fourier transform infrared spectroscopy, *Biophys. J. 78*, 1531−1540.
38. Goormaghtigh, E., Cabiaux, V., and Ruysschaert, J. M. (1994) Determination of soluble and membrane protein structure by Fourier transform infrared spectroscopy. I. Assignments and model compounds, *Subcell. Biochem. 23*, 329−362.
39. Marsh, D. (1999) Quantitation of secondary structure in ATR infrared spectroscopy, *Biophys. J. 77*, 2630−2637.
40. Zani, M. L., Pourcher, T., and Leblanc, G. (1993) Mutagenesis of acidic residues in putative membrane-spanning segments of the melibiose permease of *Escherichia coli*. II. Effect on cationic selectivity and coupling properties, *J. Biol. Chem. 268*, 3216−3221.
41. Franco, P. J., and Wilson, T. H. (1999) Arg-52 in the melibiose carrier of *Escherichia coli* is important for cation-coupled sugar transport and participates in an intrahelical salt bridge, *J. Bacteriol. 181*, 6377−6386.
42. Bassilana, M., Pourcher, T., and Leblanc, G. (1987) Facilitated diffusion properties of melibiose permease in *Escherichia coli* membrane vesicles. Release of co-substrates is rate limiting for permease cycling, *J. Biol. Chem. 262*, 16865−16870.
43. Hirai, T., and Subramaniam, S. (2004) Structure and transport mechanism of the bacterial oxalate transporter OxlT, *Biophys. J. 87*, 3600−3607.
44. Abramson, J., Smirnova, I., Kasho, V., Verner, G., Kaback, H. R., and Iwata, S. (2003) Structure and mechanism of the lactose permease of *Escherichia coli*, *Science 301*, 610−615.
45. Ding, P. Z. (2004) Loop X/XI, the largest cytoplasmic loop in the membrane-bound melibiose carrier of *Escherichia coli*, is a functional re-entrant loop, *Biochim. Biophys. Acta 1660*, 106−117.
46. Sery, N. (2002) Role of cytoplasmic loops 4−5 and 10−11 in the Na^+- symport mechanism catalyzed by the melibiose permease of *Escherichia coli*, Diploma of Advanced Studies, Nice University, France.

BI048301Z